Proceedings of the 28th IEEE
EMBS Annual International Conference
New York City, USA, Aug 30-Sept 3, 2006

A musculotendon contribution for multijoint hand control

Nick Gialias & Yoky Matsuoka

Abstract— **For multijoint arm control, intersegmental dynamic properties have been observed to play a significant role. This paper focuses on the contribution of viscoelastic musculotendon properties during coordinated hand movements. Specifically, the musculotendon passive stiffness torque is shown to be more than 90% of the total passive torque, based on two-link planar model dynamics, during repetitive hand movements. Furthermore, a large difference in the contribution to joint torque was observed depending on the relationship between wrist and finger phasic movements. With the wrist and finger in phase, the peak-to-peak stiffness torque was 24 N-cm, while it was only 6 N-cm with the wrist and finger out of phase. Despite the difference in the musculotendon dynamics between in-phase and out-of-phase coordination patterns, when they spanned similar angular excursions, the movement variance remained the same. We hypothesize that the interactive musculotendon torque contribution is accommodated by the neural controller and is utilized to achieve task-dependant impedance of the hand.**

I. Introduction

The description of multijoint dynamic movement control is complex due to the interaction of multiple segments. The major factors that contribute to the coupling of multiple limb segments are: (1) the musculotendon structures that span multiple segments and (2) link torques (T_{Link}) defined by a two-link planar model [6]. The coupled velocity and acceleration components of T_{Link}, the torques of one joint that depend on velocity and acceleration of another joint [4], have been shown to play a significant role in coordination patterns of the arm [3, 4, 6]. Studies of the arm suggest that the neural controller must either compensate for or take advantage of these torques during multijoint movement execution [4, 6]. The description of multijoint dynamic movement has largely focused on the arm and less work has focused on the hand.

For multijoint hand control, in one example, coordination patterns of the wrist and fingers have been characterized during hand drawing tasks [2]. It was shown that the preferred coordination pattern of the wrist-finger is to simultaneously flex the wrist and finger or simultaneously extend the wrist and finger (in-phase). When a circle was drawn fast, the principal axis of the circle (now an oval) tilted toward the preferred coordination pattern. When straight lines were drawn repeatedly, the lines drawn with the preferred coordination pattern had lower variance. Rather than the coupled velocity and acceleration components of link torques responsible for the arm movements, it is hypothesized that musculotendon constraints could be responsible for the observed coordination patterns. Also, models of wrist and finger coupled dynamics have been developed using combinations of translational elements and oscillators [7, 9]. The oscillatory components of these models rely on spring stiffness, a biomechanical property, to provide restoring forces.

In this paper, we further investigate the significance of musculotendon contribution during coordinated hand movements. We first show the large variation of finger passive stiffness for different wrist postures due to the musculotendon structure through static system identification. Second, the passive viscoelastic torque (T_{PVE}) and T_{Link} are separately determined for the hand (fingers and wrist). The ratio between them is compared to the literature values for elbow in-phase (IP) movements. Finally, we compared two types of hand coordination patterns (wrist and finger IP or out-of-phase (OP)) to show the difference in the magnitude of the musculotendon contribution and the relative contribution of musculotendon and link torques.

II. Methods

Four right-handed subjects (two men, two women) between the ages of 25-28 were recruited for this study from the Carnegie Mellon University student body. After receiving a brief explanation of the study, each volunteer signed an informed consent form in agreement with the university's human subject policies. All four subjects participated in both the static system identification and hand phasic experiments described below.

For both experiments, the flexion direction of the finger and wrist is considered the positive rotation direction. Zero degrees were set to be when the joint centers of elbow, wrist and MCP are aligned.

A. Static System Identification Experiment

A custom-made device was used to measure the endpoint force of the finger while rotating the finger through the entire range of motion. The index finger was constrained to only rotate at the metacarpophalangeal (MCP) joint. The proximal interphalangeal (PIP) and distal interphalangeal (DIP) joints were restrained with a finger splint. The other three fingers, thumb and palm were also restrained.

Fingertip perpendicular force was measured at 10-degree increments for three different wrist angles: 60, 0, and -60 degrees. The force values were recorded after the steady

Manuscript received April 3, 2006. This work was supported in part by NIH EB005967.

N. Gialias is in the Biomedical Engineering Department, Carnegie Mellon University, Pittsburgh, PA 15213 USA

Y. Matsuoka is in the Robotics Institute & Mechanical Engineering Department, Carnegie Mellon University, Pittsburgh, PA 15213 USA

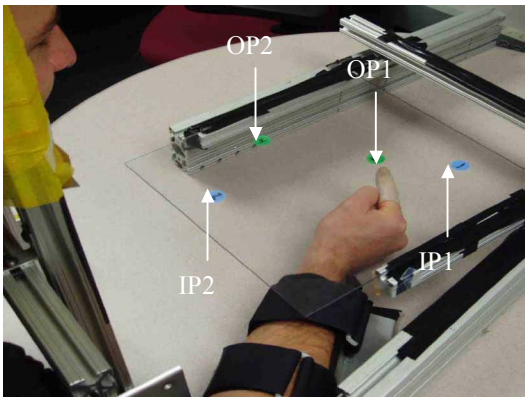

Fig. 1. Hand phasic experiment. IP1 is located at wrist angle -60 degrees and finger angle -10 degrees. OP1 is located at wrist angle -60 degrees and finger angle 80 degrees. IP2 is located at wrist angle 60 degrees and finger angle 80 degrees. OP2 is located at wrist angle 60 degrees and finger angle -10 degrees.

state value was reached for 45 seconds. Subjects were given time to rest between each of the three wrist angle conditions. The force-finger angle (θ_f) data was converted to joint torque T, and joint angular stiffness (k) was calculated.

Finger rest angle θ_{0f} was determined to be where the joint torque crossed 0 for each wrist angle. Then it was generalized to the entire range of wrist angles using a linear model. To use the angular stiffness as a function of wrist and finger angles for the hand phasic experiment, the stiffness was modeled as

$$k(\theta_f,\theta_w) = A\cdot e^{b(\theta_f-\theta_{w1})} + C\cdot e^{d(\theta_f-\theta_{w2})} \quad (1)$$

where A,b,C,d relate to the passive stiffness properties of the muscle groups of the finger and θ_{w1},θ_{w2} represent the operating range of the muscle groups. For each wrist angle, θ_w, the operating range parameters θ_{w1},θ_{w2} were determined and fit to a linear model of θ_w.

B. Hand Phasic Experiment

Hand coordination patterns were recorded using six Vicon® cameras. The subject's right forearm, PIP and DIP were restrained. The subject's head was restricted to a constant viewing angle. Targets were located on a Plexiglas™ sheet, roughly one inch over the hand (Fig 1). The In-Phase (IP) targets were placed by instructing the subject to first extend their wrist and extend their finger to a comfortable level (IP1) and then to flex their wrist and flex their finger to a comfortable level (IP2). The Out-Of-Phase (OP) targets were placed by extending their wrist and flexing their finger (OP1) and then by flexing the wrist and extending their finger (OP2).

TABLE 1
PEAK-TO-PEAK TORQUE IN N-CM: MEAN (STANDARD DEVIATION)

IP T_{ACTIVE}	IP Stiffness Torque	OP T_{ACTIVE}	OP stiffness Torque
23.3 (2.3)	23.9 (1.8)	9.8 (1.3)	5.9 (0.9)

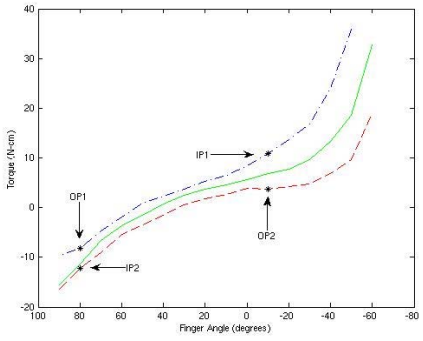

Fig. 2. Mean static system identification torque angle curve of the index finger. Targets IP1 & IP2 and OP1 & OP2 represents the two coordination patterns. Three fixed wrist angles tested: wrist extended (-.), wrist level (solid) and wrist flexed (--). Finger fully flexed is 90 degrees and finger fully extended is -60 degrees.

One cycle of movement consisted of moving from one target to another and back in 1.2 Hz (e.g. IP1 - IP2 - IP1 or OP1 – OP2 – OP1). 1.2 Hz corresponded to the fastest movement subjects could execute consistently. One trial consisted of ten cycles and a total of eight trials (four IP and four OP) were conducted for each subject. Pace of the trial was kept with a metronome and a buzzer sounded to signal the end of a trial. Subjects received feedback for the number of successful cycles executed within +/- 75msec of the target speed and turned around at +/- 1.25 cm from the center of the target.

The torque of the finger was decomposed into three components to evaluate the relative contribution of musculotendon components to active finger torque (T_{Active}). The link torque T_{Link} is based on Lagrange's equations of a two-link planar model in [6]. The passive viscoelastic torques (T_{PVE}) were composed of two components,

$$T_{PVE} = k(\theta_f - \theta_{0f}) + b\cdot\dot{\theta}_f \quad (2)$$

where $k(\theta_f - \theta_{0f})$ is the passive stiffness torque of the finger, $k(\theta_f,\theta_w)$ is finger stiffness from (1), $b\cdot\dot{\theta}_f$ is the viscous damping torque of the finger and b is the coefficient of viscous damping. The value of b =1.3 N-s/m was taken from [5] and assumed constant. The active torque of the finger was modeled as the sum of the musculotendon passive viscoelastic and link torque.

$$T_{Active} = T_{Link} + T_{PVE} \quad (3)$$

III. RESULTS

Figure 2 shows the mean results of the static system identification. All curves (corresponding to the wrist angles

TABLE 2
PEAK-TO-PEAK LINK TORQUE (N-CM) FOR DIFFERENT JOINTS AND THE PERCENTAGE OF PEAK-TO-PEAK LINK TORQUE WITH RESPECT TO THE ACTIVE TORQUE

	Elbow	Finger IP	Finger OP
T_{Link}	540	2.1	0.6
% T_{Active}	133	9.0	6.1

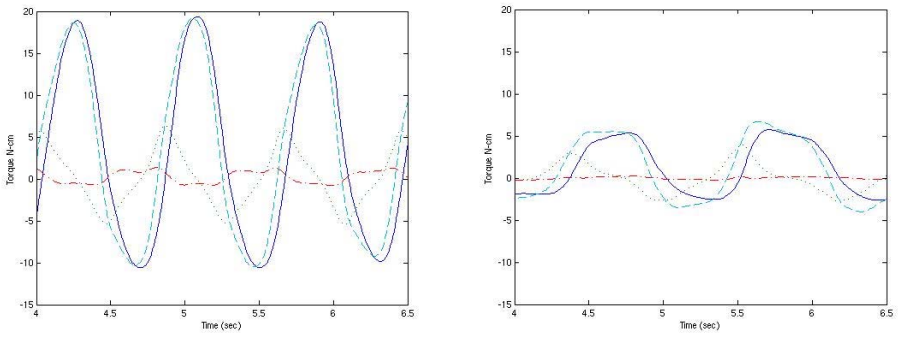

Fig. 3. Three components of finger torques for IP and OP movements. Viscous damping torque (..), link torque (-.), stiffness torque (solid) and active torque (--). **A** Torques during IP coordination pattern and **B** torques during OP coordination pattern.

60, 0, and -60 degrees) showed that torque increased with the finger angle. The finger rest angle (where the torque is 0) shifted in the direction of finger flexion as the wrist extended. The mean finger rest angle from all subjects was 26.2 (3.5 SD) degrees for wrist flexed (60 degrees), 46.9 (9.3 SD) degrees for wrist level (0 degrees), and 66.4 (10.9 SD) degrees for wrist extended (-60 degrees).

Figure 3 shows the link torque, passive viscoelastic torques and active torque from equation (3) for IP (A) and OP (B) movements. Peak-to-peak active torque was significantly larger ($p < 0.0001$) for IP than for OP due to the larger stiffness torque contribution. Four target locations related to the IP and OP movements are indicated in Fig. 2. On average, the IP movements (from IP1 to IP2) spanned a total of 23.3 (2.3 SD) N-cm in 62.5 (13.0 SD) degrees (finger), 77.7 (11.6 SD) degrees (wrist), while the OP movements (OP1 to OP2) spanned a total of 9.8 (1.3 SD) N-cm in 51.1 (12.0 SD) degrees (finger), 64.9 (8.3 SD) degrees (wrist). Table 1 shows average peak-to-peak stiffness torque and active torque for IP and OP. The passive stiffness torque for IP movements was significantly greater ($p < 0.0001$) than stiffness torque for OP movements. Stiffness torques are 11.4 times greater than link torques for IP and 9.8 times greater for OP movements.

Finger link torques were significantly smaller than published link torques for the elbow. Typical peak-to-peak link torque for the elbow were estimated from [1]. Table 2 shows peak-to-peak link torques for the elbow and finger and the relative percent contribution to the active torque. When the percentage is larger than 100%, it means that the peak-to-peak link torque was larger than the peak-to-peak active torque. Elbow link torque, position and velocity were estimated from [1] and elbow stiffness and damping were taken from [10].

Figure 4 shows typical movement trajectories during one trial in extrinsic fingertip (A) and joint (B) space. To describe the movement variance, the location where the peak velocity was experienced was identified. Table 3 shows the mean location and its variance where the peak velocity was experienced for each subject.

IV. Discussion

The objective of these experiments was to investigate the musculotendon influence on multijoint hand movements. We first demonstrated that multijoint hand dynamics are affected by the passive musculotendon stiffness properties significantly more than the multijoint arm dynamics. For example, the elbow joint working in a plane parallel to the floor could rest at a variety of angles. This is because the imbalance in the flexor and extensor muscle passive tensions does not overcome the joint friction and the inertia of the forearm to cause the restoring movement. For the hand, the total mass is small with respect to the amount of torque due to multi-articular tendons that causes the imbalance between flexors and extensors. Figure 3 showed that the link torque, which consists of the inertial and interactive terms, is negligible compared to the musculotendon contributions to the active torque.

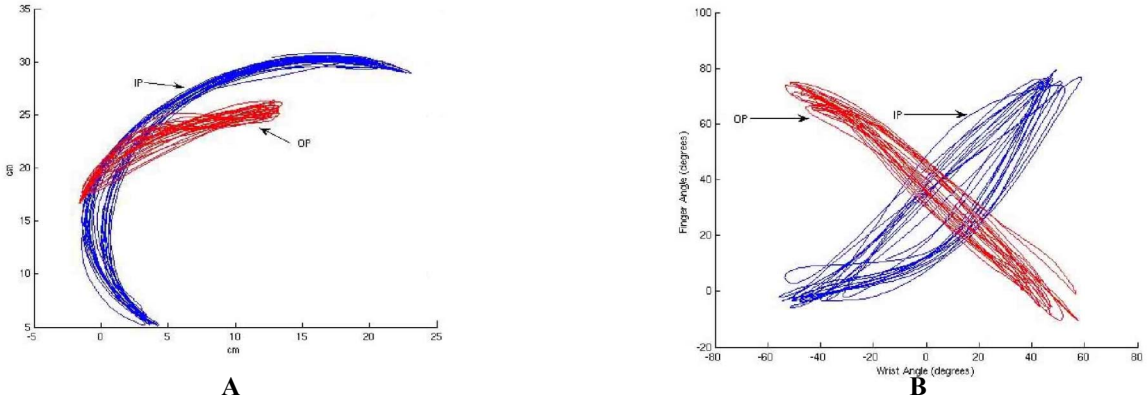

Fig. 4. An example of IP and OP trajectories and joint angle excursions for typical trials. Each trial consisted of 10 movement cycles executed at 1.2 Hz. **A** finger endpoint trajectory and **B** finger and wrist angles

TABLE 3
MEAN LOCATION (IN CM FOR EXTRINISC, LABELED XY, AND DEGREES FOR JOINT SPACE, LABELED W/F) WHERE THE PEAK VELOCITY WAS FOUND FOR EACH SUBJECT AND STANDARD DEVIATION (IN PARENTHESES)

Subject	IP flex xy	OP flex xy	IP ext xy	OP ext xy	IP flex w/f	OP flex w/f	IP ext w/f	OP ext xy
M1	8.3	6.9	4.5	6.2	135	118	135	6.2
	(2.1)	(.3)	(.2)	(.3)	(4)	(14)	(8)	(.3)
M2	11.4	10.3	11.5	10.7	119	143	126	10.7
	(1.2)	(.1)	(.7)	(.3)	(4)	(3)	(23)	(.3)
F1	2.5	1.8	3.8	2.6	118	125	126	2.6
	(.5)	(.1)	(1.0)	(.9)	(5)	(74)	(21)	(.9)
F2	2.5	1.8	3.8	2.5	119	125	125	2.5
	(.5)	(.1)	(1.0)	(.8)	(5)	(65)	(27)	(.8)
pvalue	0.072		0.25		0.41		0.54	

Second, we demonstrated that hand movements with similar range of joint angles could have dramatically different stiffness torques depending on the phase between the wrist and finger movements. The increased finger stiffness when the wrist is moving in-phase (IP movements) is due to the musculotendon arrangement of the hand. The extrinsic muscles in the forearm actuate the finger via long tendons that pass over the wrist (not through the center) [8]. Therefore, when the wrist angle is varied, the tendon lengths of the extrinsic muscles also change. The change in muscle length causes the rest angle of the finger to shift as seen in Figure 2. Figure 2 also highlights the difference between the IP and OP movements in passive stiffness contribution. The IP movements (between IP1 and IP2) span a larger range of torques than the OP movements (between OP1 and OP2), while spanning similar angular excursions. As a result, the IP movements experience a larger range of stiffness torque. To accommodate this wide range of stiffness torque, a modulation of neural strategy is required to produce consistent behavior of the hand.

It is interesting to note that there was no noticeable difference in movement trajectory variance for the two coordination patterns tested. The previous literature [2] showed that OP movements have larger movement variance. There are multiple possibilities for the difference in our results. First, in our experiment, the IP and OP movements spanned a similar range of joint angles. To produce movements that are the same size in the extrinsic space (as done previously) require more joint movements for the OP than IP movements. It is possible that the movement variability is associated with the total joint excursion, not the fingertip excursion. Another possibility for the difference in our results is that our experiment did not require subjects to hold onto a pen. Subjects executed movements by using their fingertip to move from one target to another. It is possible that when the hand is under a constraint where the muscles are already co-activated to hold onto a pen, it is optimal to activate all the flexors together and then all the extensors together (as for the IP movements).

Finally, we are interested in observing the modulation of hand stiffness during different manipulation tasks. Given the significance and the wide range of stiffness torque in multijoint hand dynamics, we predict that the nervous system utilizes this property to accomplish tasks. It is possible that the preferred coordination patterns (IP movements) seen previously may be related to the modulation of task-dependant stiffness to stabilize the movements without having to increase cocontraction or rely on slow feedback information.

REFERENCES

[1] Dounskaia NV, Swinnen SP, Walter CB, Spaepen AJ, Verschueren SM. Hierarchical control of different elbow-wrist coordination patterns. Exp Brain Res. 1998 Aug;121(3):239-54.

[2] Dounskaia N, Ketcham CJ, Stelmach GE. Commonalities and differences in control of various drawing movements. Exp Brain Res. 2002 Sep;146(1):11-25.

[3] Dounskaia N, Wisleder D, Johnson T. Influence of biomechanical factors on substructure of pointing movements. Exp Brain Res. 2005 Aug;164(4):505-16.

[4] Gribble PL, Ostry DJ. Compensation for interaction torques during single- and multijoint limb movement. J Neurophysiol. 1999 Nov;82(5):2310-26.

[5] Hajian AZ (1997). "A characterization of the mechanical impedance of human hands" Ph.D Thesis Harvard University

[6] Hollerbach JM, Flash T. Dynamic interactions between limb segments during planar arm movement. Biological Cybernetics, 1982 44, 67-77.

[7] Hollerbach, JM. An oscillation theory of handwriting. Biol. Cybern., 1981 39:139-156

[8] Knutson JS, Kilgore KL, Mansour JM, Crago PE. Intrinsic and extrinsic contributions to the passive moment at the metacarpophalangeal joint. J Biomech. 2000 33(12):1675-81.

[9] Singer Y, Tishby N. Dynamical encoding of cursive handwriting. Biol Cybern. 1994;71(3):227-37.

[10] MacKay WA, Crammond DJ, Kwan HC, Murphy JT. Measurements of human forearm viscoelasticity. J Biomech. 1986 19(3):231-238